Journal of the Egyptian Mathematical Society (2016) **24**, 471–478

Egyptian Mathematical Society

Journal of the Egyptian Mathematical Society

www.etms-eg.org
www.elsevier.com/locate/joems

Unsteady MHD free convection flow with Hall effect of a radiating and heat absorbing fluid past a moving vertical plate with variable ramped temperature

G.S. Seth, B. Kumbhakar*, R. Sharma

Department of Applied Mathematics, Indian School of Mines, Dhanbad 826004, India

Received 25 August 2014; revised 1 June 2015; accepted 30 July 2015
Available online 29 October 2015

Keywords

Free convection;
MHD;
Heat absorption;
Hall current;
Variable ramped temperature

Abstract Unsteady hydromagnetic free convection flow of a viscous, incompressible, electrically conducting, optically thick radiating and heat absorbing fluid past an accelerated moving vertical plate with variable ramped temperature is investigated. Exact solution of the governing equations for the fluid velocity and fluid temperature are obtained by Laplace transform technique. The numerical values of primary and secondary fluid velocities and fluid temperature are displayed graphically whereas those of shear stress and rate of heat transfer at the plate are presented in tabular form for various values of pertinent flow parameters.

2010 MATHEMATICS SUBJECT CLASSIFICATION: 76R10; 76W05; 60J70; 81V70

1. Introduction

Effect of thermal radiation on hydromagnetic free convection flow plays an important role in several scientific and industrial processes such as high temperature casting and levitation, thermo-nuclear fusion, furnace design, glass production, solar power technology etc. It may be mentioned here that, unlike convection/conduction problems, the governing equations for fluid flow problems considering the effect of thermal radiation become quite complicated and hence many difficulties arise while solving such equations. So, a reasonable approximation (Rosseland approximation) to the radiative term is used to solve those equations for optically thick fluid. Detailed explanation about radiative heat transfer and its applications may be found in well documented text book by Howell et al. [1]. Moreover, combined effects of thermal radiation and heat generation/absorption on hydromagnetic free convection flow is of considerable importance for many scientific and engineering

* Corresponding author. Tel.: +91 9570216865.
E-mail addresses: gsseth_ism@yahoo.com (G.S. Seth), bidya.ism@gmail.com (B. Kumbhakar), rohit.iitg08@gmail.com (R. Sharma).
Peer review under responsibility of Egyptian Mathematical Society.

Production and hosting by Elsevier

http://dx.doi.org/10.1016/j.joems.2015.07.007

applications viz. heating and cooling of chambers, fossil fuel combustion energy processes, evaporation from large open water reservoirs, propulsion devices for aircraft, missiles, satellites and space vehicles etc. Keeping in mind the importance of such applications, combined effects of thermal radiation and heat generation/absorption in hydromagnetic boundary layer flow of an optically thick fluid past a vertical plate/stretching surface is investigated by several researchers considering different aspects of the problem. Mentioned may be made of research studies of Chamkha [2], Elbashbeshy and Emam [3], Pal [4] and Makinde [5].

In fact, free convection flows are generally modeled by the researchers under the assumptions of constant surface temperature or constant surface heat flux. But, in many physical situations, the temperature of bounding surface may require non-uniform or arbitrary surface temperature. Moreover, there may be step discontinuities in the surface temperature or ramped surface temperature (Chandran et al. [6]). Keeping in view this fact, several researchers investigated free convection from a vertical plate with ramped temperature considering various aspects of the problem. Some of relevant research studies are due to Rajesh [7], Samiulhaq et al. [8], Das [9], Nandkeolyar and Das [10], Nandkeolyar et al. [11], Kundu et al. [12] and Seth et al. [13].

Further, it is well known that in an ionized fluid, where density is low and/or magnetic field is strong, the effect of Hall current become significant. Moreover, it has a tendency to induce secondary flow in the flow-field. Therefore, it seems to be significant to study its effect on the flow-field. Hall effect on fluid flow find applications in MHD power generators, Hall current accelerators, nuclear power reactors, magnetometers, underground energy storage system, Hall effect sensors, spacecraft propulsion etc. Keeping in mind this fact, Pop and Watanabe [14], Aboeldahab and Elbarbary [15], Seth et al. [16] and Das et al. [17] studied the effect of Hall current on hydromagnetic flow past a vertical plate considering different aspects of the problem.

However, in all the investigations carried out by researchers considering ramped temperature profiles, the interval for rampedness with respect to time in the plate temperature is assumed fixed i.e. $0 < t' \leq t_0$($t'$and t_0 are time and characteristic time respectively) which reduces to $0 < t \leq 1$(t being the dimensionless time) in non-dimensional form. It is to be noted that interval for ramped profile varies from material to material depending upon the specific heat capacity of the material. To the authors' knowledge no researcher has yet investigated the problem considering variable ramped temperature within the plate. Variable ramped temperature profiles appear in real world situation in building air-conditioning systems, fabrication of thin-film photovoltaic devices, phase transition in processing of materials, turbine blade heat transfer, heat exchangers etc.

Aim of the present investigation is to study unsteady hydromagnetic free convection flow with Hall effects of a viscous, incompressible, electrically conducting, optically thick radiating and heat absorbing fluid past an accelerated moving vertical plate with variable ramped temperature. In this study we have considered t_0 as critical time for rampedness in place of characteristic time. Due to this reason, in our study, the interval for rampedness becomes $0 < t \leq t_1$ (t_1 being the dimensionless critical time for rampedness) whereas in the above mentioned research studies the interval for rampedness is $0 < t \leq 1$ in non-dimensional form. It may be noted that the physical meaning of critical time for rampedness is the time when plate temperature changes form ramped temperature to uniform temperature.

Nomenclature

B_0	uniform magnetic field
c_p	specific heat at constant pressure
g	acceleration due to gravity
G_r	thermal Grashof number
k	thermal conductivity of the fluid
k^*	mean absorption coefficient
m	Hall current parameter
M^2	magnetic parameter
N_r	radiation parameter
P_r	Prandtl number
Q_0	heat absorption coefficient
q_r	radiative heat flux
t'	time
t_0	critical time for rampedness
t_1	dimensionless critical time for rampedness
T'	fluid temperature
U_0	characteristic velocity
u'	fluid velocity in x'-direction
w'	fluid velocity in z'-direction

Greek Symbols

β	coefficient of thermal expansion
η	non-dimensional space variable
σ^*	Stefan Boltzmann constant
σ	electrical conductivity
ρ	fluid density
ν	kinematic coefficient of viscosity
ω_e	cyclotron frequency
τ_e	electron collision time
φ	heat absorption parameter

Subscripts

w	condition at the wall
∞	free-stream condition/ Initial condition at the wall

2. Formulation of the problem and its solution

Consider unsteady hydromagnetic free convection flow of a viscous, incompressible, electrically conducting, optically thick radiating and heat absorbing fluid past a moving infinite vertical flat plate with variable ramped temperature. We choose the Cartesian coordinate system (x', y', z') in such a way that x'-axis is along the vertical plate in upward direction, y'-axis is normal to the plane of the plate directed into the fluid region and z'-axis is normal to $x'y'$-plane. A uniform transverse magnetic field of strength B_0 is applied in a direction parallel to y'-axis. Initially, i.e. at time $t' \leq 0$, both the plate and surrounding fluid are at rest and maintained at uniform temperature T'_∞. At time $t' > 0$, the plate starts moving along x' direction with a velocity $U(t') = a't'$(a' being arbitrary constant) and at the same time temperature of the plate is raised to $T'_\infty + (T'_w - T'_\infty)(t'/t_0)$ when $0 < t' \leq t_0$ and it is maintained at uniform temperature

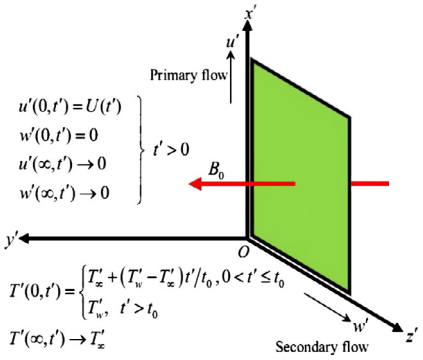

Fig. 1. Physical model of the problem.

T'_w when $t' > t_0(t_0$ being critical time for rampedness). Physical model of the problem is shown in Fig. 1.

Since plate is of infinite extent along x' and z' directions, all the physical quantities except pressure depend on y' and t' only. Induced magnetic field produced by fluid motion is neglected in comparison to applied one. This is justified because magnetic Reynolds number is very small for liquid metals and partially ionized fluids which are commonly used in various industrial processes (Cramer and Pai [18]). Since no external electric field is applied into the flow-field so the effect of polarization of fluid is negligible which corresponds to the case where no energy is added or extracted from the fluid by electrical means (Cramer and Pai [18]).

With the assumptions made above, the governing equations for the fluid flow problem taking Hall current into account, under Boussinesq approximation, are given by

$$\frac{\partial u'}{\partial t'} = \nu\frac{\partial^2 u'}{\partial y'^2} - \frac{\sigma B_0^2}{\rho(1+m^2)}(u' + mw') + g\beta(T' - T'_\infty), \tag{2.1}$$

$$\frac{\partial w'}{\partial t'} = \nu\frac{\partial^2 w'}{\partial y'^2} + \frac{\sigma B_0^2}{\rho(1+m^2)}(mu' - w'), \tag{2.2}$$

$$\frac{\partial T'}{\partial t'} = \frac{k}{\rho c_p}\frac{\partial^2 T'}{\partial y'^2} - \frac{Q_0}{\rho c_p}(T' - T'_\infty) - \frac{1}{\rho c_p}\frac{\partial q_r}{\partial y'}. \tag{2.3}$$

Initial and boundary conditions to be satisfied are

$$t' \le 0 \ : \ u' = 0, \quad w' = 0, \quad T' = T'_\infty \quad \text{for all } y' \ge 0, \tag{2.4a}$$

$$t' > 0 \ : \ u' = a't', \ w' = 0,$$
$$T' = \begin{cases} T'_\infty + (T'_w - T'_\infty)t'/t_0 & \text{at } y' = 0 \text{ when } 0 < t' \le t_0, \\ T'_w & \text{at } y' = 0 \text{ when } t' > t_0 \end{cases} \tag{2.4b}$$

$$t' > 0 \ : u' \to 0, \ w' \to 0, \ T' \to T'_\infty \text{ as } y' \to \infty. \tag{2.4c}$$

For an optically thick gray fluid, the radiative heat flux q_r is approximated by Rosseland approximation (Howell et al. [1]) which is given by

$$q_r = -\frac{4\sigma^*}{3k^*}\frac{\partial T'^4}{\partial y'}. \tag{2.5}$$

It is assumed that the temperature difference between fluid in the boundary layer region and free-stream is very small so that T'^4 may be expressed as a linear function of temperature T'. Expanding T'^4 in Taylor series about T'_∞ and neglecting second and higher order terms, we obtain

$$T'^4 \cong 4T'^3_\infty T' - 3T'^4_\infty. \tag{2.6}$$

Using Eqs. (2.5) and (2.6) in Eq. (2.3), we obtain

$$\frac{\partial T'}{\partial t'} = \frac{k}{\rho c_p}\left(1 + \frac{16\sigma^* T'^3_\infty}{3kk^*}\right)\frac{\partial^2 T'}{\partial y'^2} - \frac{Q_0}{\rho c_p}(T' - T'_\infty). \tag{2.7}$$

We introduce following non-dimensional quantities and flow parameters to present Eqs. (2.1), (2.2) and (2.7) along with initial and boundary conditions (2.4a)–(2.4c) in non-dimensional form

$$\left.\begin{aligned} &\eta = U_0 y'/\nu, \ \ t = U_0^2 t'/\nu, \ \ u = u'/U_0, \ \ w = w'/U_0, \\ &T = (T' - T'_\infty)/(T'_w - T'_\infty), \\ &G_r = \nu g\beta(T'_w - T'_\infty)/U_0^3, \ \ M^2 = \sigma B_0^2\nu/\rho U_0^2, \\ &N_r = 16\sigma^* T'^3_\infty/3kk^*, \\ &P_r = \rho\nu c_p/k, \ \ t_1 = U_0^2 t_0/\nu, \ \ \varphi = Q_0\nu/\rho c_p U_0^2. \end{aligned}\right\} \tag{2.8}$$

Making use of (2.8), Eqs. (2.1), (2.2) and (2.7), in non-dimensional form, reduce to

$$\frac{\partial F}{\partial t} + \frac{M^2(1 - im)}{1 + m^2}F = \frac{\partial^2 F}{\partial \eta^2} + G_r T, \tag{2.9}$$

$$\frac{\partial T}{\partial t} = (1 + N_r)\frac{1}{P_r}\frac{\partial^2 T}{\partial \eta^2} - \varphi T, \tag{2.10}$$

where $F(\eta, t) = u(\eta, t) + iw(\eta, t)$.

Initial and boundary conditions (2.4a)–(2.4c), in non-dimensional form, are given by

$$t \le 0 \quad : \ F = 0, \quad T = 0 \quad \text{for all } \eta \ge 0, \tag{2.11a}$$

$$t > 0 \quad : \ F = at, \quad T = \begin{cases} t/t_1 & \text{at } \eta = 0 \text{ for } 0 < t \le t_1, \\ 1 & \text{at } \eta = 0 \text{ for } t > t_1, \end{cases} \tag{2.11b}$$

$$t > 0 \quad : F \to 0, \quad T \to 0 \quad \text{as } \eta \to \infty, \tag{2.11c}$$

where $a = a'\nu/U_0^3$ is a non-dimensional constant.

It is evident from Eqs. (2.9) and (2.10) that energy Eq. (2.10) is uncoupled from momentum Eq. (2.9). Using Laplace transform technique, first the solution for fluid temperature $T(\eta, t)$ is obtained by solving Eq. (2.10) subject to the initial and boundary conditions (2.11a)–(2.11c) and then using this solution in Eq. (2.9), solution for fluid velocity $F(\eta, t)$ is obtained. The exact solutions for fluid temperature $T(\eta, t)$ and fluid velocity $F(\eta, t)$ are obtained and expressed in the following simplified form:

$$T(\eta, t) = (1/2t_1)[T_1(\eta, t) - H(t - t_1)T_1(\eta, t - t_1)], \tag{2.12}$$

$$F(\eta, t) = (1/2)\big[aF_1(\eta, t) + (G_r^*/\lambda_3^2 t_1)\{F_2(\eta, t) - H(t - t_1)F_2(\eta, t - t_1)\}\big], \tag{2.13}$$

where $T_1(\eta, t) = (t + \alpha_1)\exp(\beta_1\eta)erfc(\gamma_1 + \delta_1) + (t - \alpha_1)\exp(-\beta_1\eta)erfc(\gamma_1 - \delta_1)$,

$$F_1(\eta, t) = (t + \alpha_2)\exp(\beta_2\eta)erfc(\gamma_2 + \delta_2) + (t - \alpha_2)\exp(-\beta_2\eta)erfc(\gamma_2 - \delta_2),$$

$$
\begin{aligned}
&F_2(\eta, t)\\
&= \exp(\lambda_3 t)\{\exp(\beta_3\eta)erfc(\gamma_1+\delta_3)\\
&\quad + \exp(-\beta_3\eta)erfc(\gamma_1-\delta_3) - \exp(\beta_4\eta)erfc(\gamma_2+\delta_4)\\
&\quad - \exp(-\beta_4\eta)erfc(\gamma_2-\delta_4)\} - \lambda_3\{(t+1/\lambda_3+\alpha_1)\exp(\beta_1\eta)\\
&\quad \times erfc(\gamma_1+\delta_1) + (t+1/\lambda_3-\alpha_1)\exp(-\beta_1\eta)erfc(\gamma_1-\delta_1)\\
&\quad -(t+1/\lambda_3+\alpha_2)\exp(\beta_2\eta)erfc(\gamma_2+\delta_2) - (t+1/\lambda_3-\alpha_2)\\
&\quad \times \exp(\beta_2\eta)erfc(\gamma_2-\delta_2)\},
\end{aligned}
$$

$$
\begin{aligned}
&\alpha_1 = (\eta/2)(\lambda_2/\phi)^{1/2},\ \alpha_2 = \eta/2\lambda_1^{1/2},\ \beta_1 = (\lambda_2\phi)^{1/2},\ \beta_2 = \lambda_1^{1/2},\\
&\beta_3 = \{\lambda_2(\phi+\lambda_3)\}^{1/2},\ \beta_4 = (\lambda_1+\lambda_3)^{1/2},\\
&\gamma_1 = (\eta/2)(\lambda_2/t)^{1/2},\ \gamma_2 = \eta/2t^{1/2},\ \delta_1 = (\phi t)^{1/2},\ \delta_2 = (\lambda_1 t)^{1/2},\\
&\delta_3 = \{(\phi+\lambda_3)t\}^{1/2},\ \delta_4 = \{(\lambda_1+\lambda_3)t\}^{1/2},\\
&\lambda_1 = M^2/(1+m^2) - imM^2/(1+m^2),\ \lambda_2 = \mathrm{P}r/(1+N_r),\\
&\lambda_3 = (\lambda_2\varphi-\lambda_1)/(1-\lambda_2),\ G_r^* = G_r/(1-\lambda_2).
\end{aligned}
$$

Here $H(t-t_1)$ and $erfc(x)$ are, respectively, Heaviside unit step function and complementary error function.

3. Rate of heat transfer at the plate

Expression for rate of heat transfer at the plate i.e. $(\partial T/\partial\eta)_{\eta=0}$ is presented in the following simplified form for both ramped temperature and isothermal plates.

$$(\partial T/\partial\eta)_{\eta=0} = (1/t_1)[T_2(0,t) - H(t-t_1)T_2(0,t-t_1)], \qquad (3.1)$$

where $T_2(0,t) = -(\lambda_2 t/\pi)^{1/2}\exp(-\delta_1^2) - (t+1/2\varphi)\beta_1\, erf(\delta_1)$.

4. Shear stress at the plate

Expressions for shear stress at the plate due to primary and secondary flows respectively i.e. τ_x and τ_z are presented in the following simplified form

$$\tau_x + i\tau_z = a\,F_3(0,t) + (G_r^*/\lambda_3^2 t_1)\{F_4(0,t) - H(t-t_1)F_4(0,t-t_1)\}, \qquad (4.1)$$

where $F_3(0,t) = -\sqrt{t/\pi}\exp(-\delta_2^2) - (t+1/2\beta_2^2)\beta_2\, erf(\delta_2)$,

$$
\begin{aligned}
F_4(0,t) = \lambda_3\big[&\sqrt{t/\pi}\,\{\sqrt{\lambda_2}\exp(-\delta_1^2) - \exp(-\delta_2^2)\} + (t+1/\lambda_3\\
&+1/2\varphi)\beta_1\, erf(\delta_1)\\
&-(t+1/\lambda_3+1/2\lambda_1)\beta_2\, erf(\delta_2)\big] - \exp(\lambda_3 t)\{\beta_3\, erf(\delta_3)\\
&-\beta_4\, erf(\delta_4)\}.
\end{aligned}
$$

5. Validation of the solution

When the critical time for rampedness $t_1 = 1$ or length of the interval for rampedness is $0 < t \le 1$, we have compared the present numerical results for fluid temperature and fluid velocity in the absence of Hall current ($m = 0$) and thermal radiation ($N_r = 0$) with those of Seth et al. [13] for non-porous medium and without solutal buoyancy force. Our results are in excellent agreement with the results obtained by Seth et al. [13] which is clearly evident from Figs. 2 and 3.

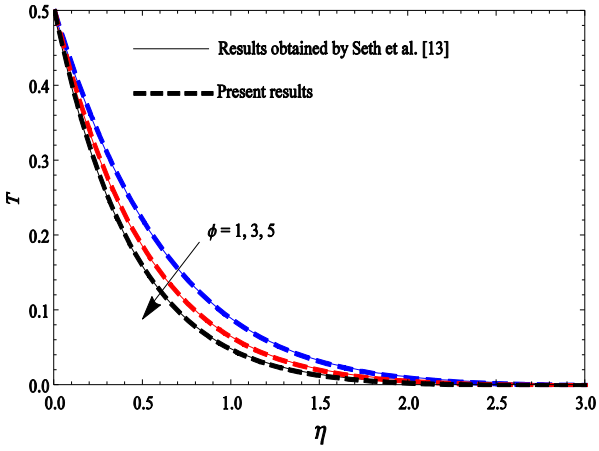

Fig. 2. Temperature profiles when $N_r = 0$, $t = 0.5$ and $P_r = 0.71$.

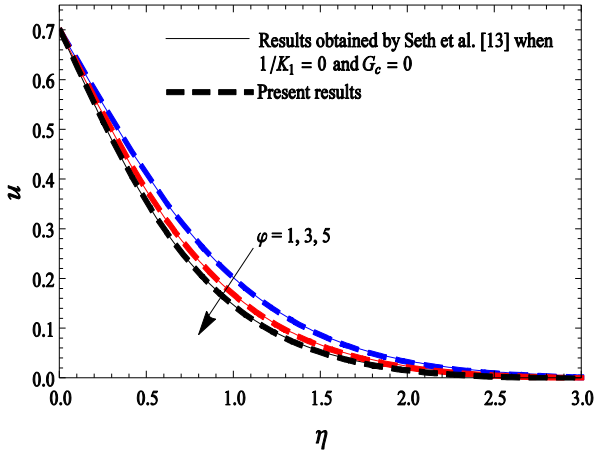

Fig. 3. Velocity profiles when $m = 0$, $M^2 = 4$, $G_r = 6$, $N_r = 0$, $t = 0.7$, $a = 1$ and $P_r = 0.71$.

6. Results and discussion

In order to analyze the effect of critical time for rampedness, thermal radiation and time on the temperature field, numerical values of fluid temperature T, computed from the analytical solution (2.12), are shown graphically versus boundary layer coordinate η in Figs. 4–6 for various values of critical time for rampedness t_1, radiation parameter N_r and time t taking heat absorption parameter $\varphi = 3$ and Prandtl number $P_r = 0.71$ (ionized air). Fig. 4 illustrates the effect of critical time for rampedness on fluid temperature. It is evident from Fig. 4 that T decreases on increasing t_1. This implies that, fluid temperature is getting reduced on increasing critical time for rampedness. Figs. 5 and 6 depict the influence of thermal radiation and time on fluid temperature. It is evident from Figs. 5 and 6 that T increases on increasing N_r and t. This implies that thermal radiation tends to enhance fluid temperature. Fluid temperature is getting enhanced with the progress of time. It is evident form Fig. 6 that plate temperature increases on increasing time up to $t \le t_1$. When $t > t_1$ plate temperature becomes uniform and is equal to 1 which is in agreement with the condition (2.11b). As we know that for isothermal plate, temperature of the plate is uniform, i.e. in non-dimensional form fluid temperature $T = 1$ at the plate for every values of time t. This means that nature

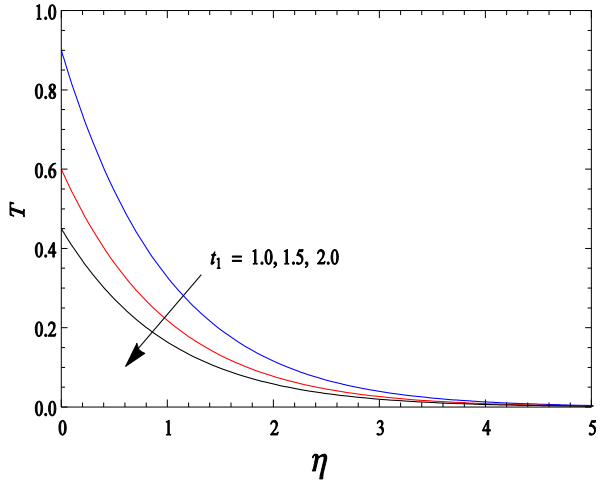

Fig. 4. Temperature profiles when $N_r = 2$ and $t = 0.9$.

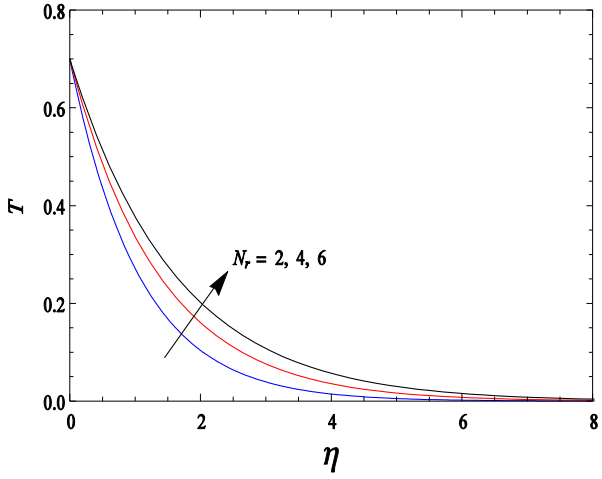

Fig. 5. Temperature profiles when $t_1 = 2$ and $t = 1.4$.

of fluid temperature is same for both ramped temperature and isothermal plate when $t > t_1$. However, fluid temperature is getting enhanced in the flow-field whether $t \leq t_1$ or $t > t_1$. But temperature filed approaches to steady state when $t \geq 3.2$. It is also observed from Figs. 4–6 that the thickness of thermal boundary layer increases on increasing N_r and t whereas it decreases on increasing t_1.

To study the influence of magnetic field, Hall current, thermal buoyancy force, critical time for rampedness, thermal radiation and time on the flow-field, numerical values of primary fluid velocity u and secondary fluid velocity w within the boundary layer region, computed from the analytical solution (2.13), are displayed graphically versus boundary layer coordinate η in Figs. 7–12 for various values of M^2, m, G_r, t_1, N_r and t taking $a = 1$, $\varphi = 3$ and $P_r = 0.71$. Fig. 7 depicts the influence of magnetic field on the primary and secondary fluid velocities. It is revealed from Fig. 7 that u and w decrease on increasing M^2. This implies that magnetic field tends to decelerate fluid flow in both the primary and secondary flow directions throughout the boundary layer region. This is due to the fact that application of a magnetic field to an electrically conducting fluid gives rise to a mechanical force, called Lorentz force, which has a tendency to resist fluid motion in the flow-field. Fig. 8 illustrates

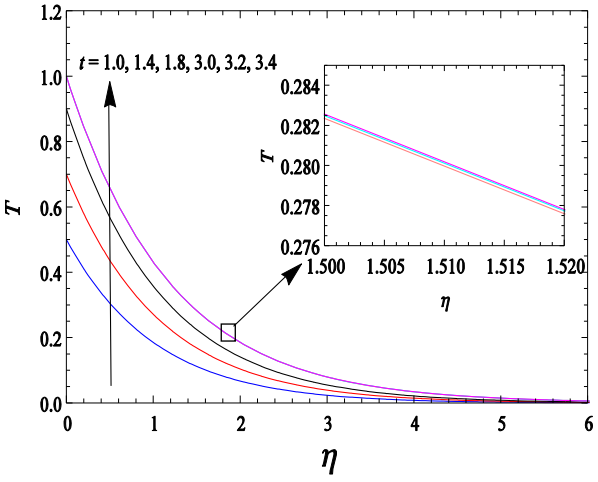

Fig. 6. Temperature profiles when $t_1 = 2$ and $N_r = 2$.

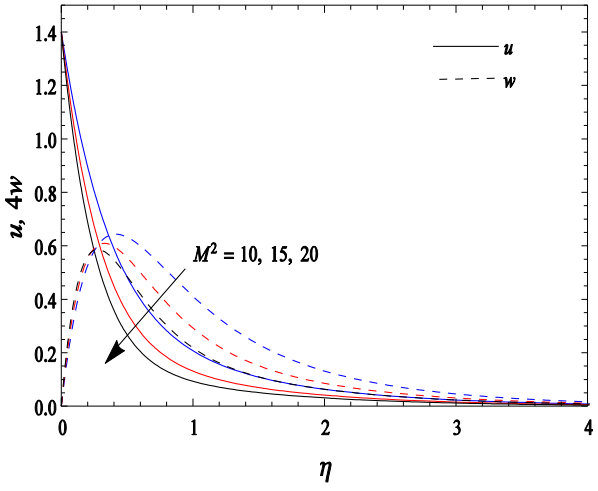

Fig. 7. Velocity profiles when $m = 0.5$, $G_r = 6$, $t_1 = 2$, $N_r = 2$ and $t = 1.4$.

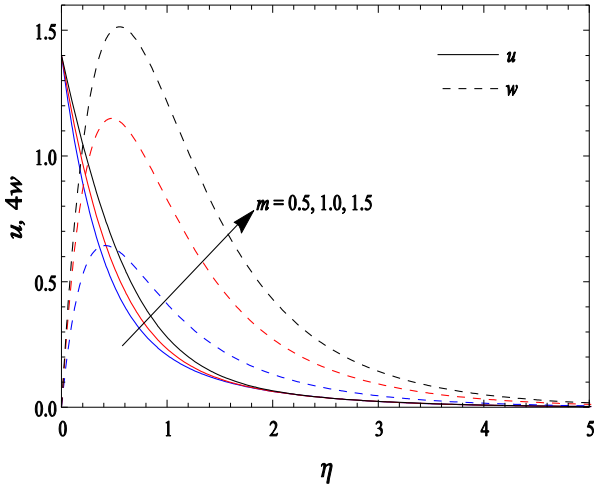

Fig. 8. Velocity profiles when $M^2 = 10$, $G_r = 6$, $t_1 = 2$, $N_r = 2$ and $t = 1.4$.

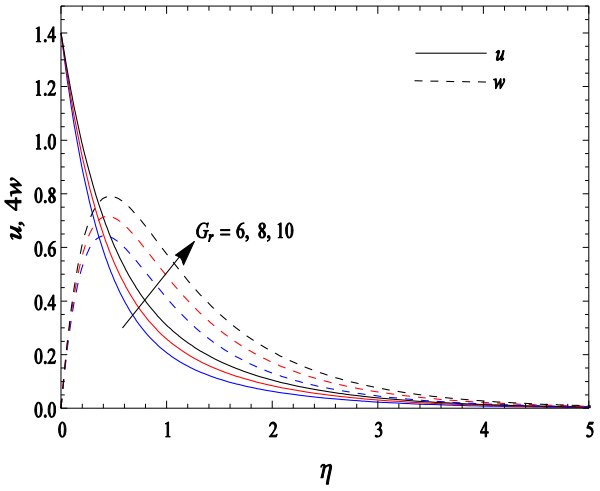

Fig. 9. Velocity profiles when $M^2 = 10$, $m = 0.5$, $t_1 = 2$, $N_r = 2$ and $t = 1.4$.

the effect of Hall current on the primary and secondary fluid velocities. It is evident form Fig. 8 that u and w increase on increasing m. This implies that Hall current tends to accelerate fluid flow in both the primary and secondary flow directions throughout the boundary layer region. This is due to the reason that Hall current induces secondary flow in the flow-field. Fig. 9 presents the influence of thermal buoyancy force on the primary and secondary fluid velocities. It is noticed from Fig. 9 that u and w increase on increasing G_r. G_r measures the relative strength of thermal buoyancy force to viscous force, an increase in G_r leads to an increase in thermal buoyancy force. Since, fluid flow in this problem is induced due to free convection arising as a result of thermal buoyancy force, therefore, thermal buoyancy force will obviously tend to accelerate fluid flow in both the primary and secondary flow directions throughout the boundary layer region. Fig. 10 demonstrates the effect of critical time for rampedness on the primary and secondary fluid velocities. It is evident from Fig. 10 that u and w decrease on increasing t_1. This implies that fluid flow in both the primary and secondary flow directions is getting decelerated with the increase in critical time for rampedness throughout the boundary layer region. This is because an increase in t_1 leads to decrease in fluid temperature (see Fig. 4) and, therefore, effect of thermal buoyancy force is reduced. Consequently, fluid velocity decreases throughout the boundary layer region. Fig. 11 exhibits the effect of thermal radiation on the primary and secondary fluid velocities. It is observed from Fig. 11 that u and w increase on increasing N_r. This implies that thermal radiation tends to accelerate fluid flow in both the primary and secondary flow directions throughout the boundary layer region. This happens because thermal radiation has a tendency to enhance fluid temperature (see Fig. 5) which results in the increase of thermal buoyancy force. Fig. 12 illustrates the influence of time on the primary and secondary fluid velocities. It is perceived from Fig. 12 that u and w increase on increasing t. This implies that fluid flow is getting accelerated in both the primary and secondary flow directions throughout the boundary layer region with the progress of time. This may be due to rise in fluid temperature with the progress of time (see Fig. 6) which results in enhancement of thermal buoyancy force. It is also noticed form Fig. 12 that primary and secondary velocity profiles are becoming closer as time progresses when $t > t_1$.

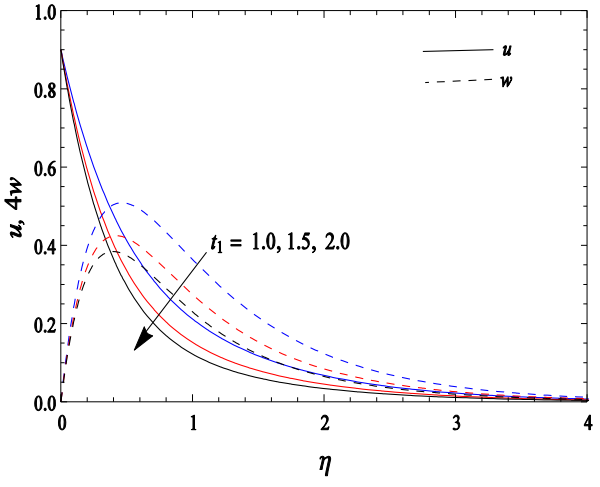

Fig. 10. Velocity profiles when $M^2 = 10$, $m = 0.5$, $G_r = 6$, $N_r = 2$ and $t = 0.9$.

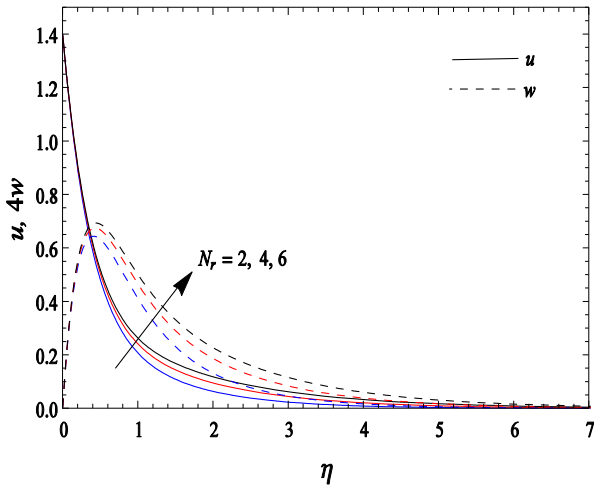

Fig. 11. Velocity profiles when $M^2 = 10$, $m = 0.5$, $G_r = 6$, $t_1 = 2$ and $t = 1.4$.

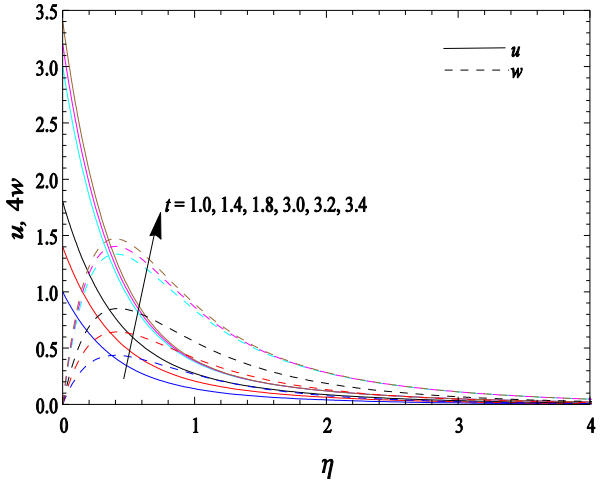

Fig. 12. Velocity profiles when $M^2 = 10$, $m = 0.5$, $G_r = 6$, $t_1 = 2$ and $N_r = 2$.

Table 1 Rate of heat transfer at the plate when $t_1 = 2$ and $t = 1.4$.

	$-(\partial T/\partial\eta)_{\eta=0}$		
$N_r \downarrow$ $\varphi \rightarrow$	1	3	5
2	0.4586	0.6600	0.8159
4	0.3553	0.5112	0.6320
6	0.3002	0.4321	0.5341

Table 2 Rate of heat transfer at the plate when $\varphi = 3$ and $t = 0.9$.

	$-(\partial T/\partial\eta)_{\eta=0}$		
$t_1 \downarrow$ $N_r \rightarrow$	2	4	6
1.0	0.8982	0.6957	0.5880
1.5	0.5988	0.4638	0.3920
2.0	0.4491	0.3479	0.2940

Table 3 Rate of heat transfer at the plate when $t_1 = 2$ and $N_r = 2$.

	$-(\partial T/\partial\eta)_{\eta=0}$		
$t \downarrow$ $\varphi \rightarrow$	1	3	5
1.0	0.3580	0.4913	0.5983
1.4	0.4586	0.6600	0.8159
1.8	0.5576	0.8286	1.0334
3.0	0.4930	0.8428	1.0878
3.2	0.4911	0.8427	1.0878
3.4	0.4898	0.8427	1.0878

This means that both the primary and secondary velocities approach steady state with the progress of time when $t > t_1$. It is observed from Figs. 7–12 that secondary fluid velocity attains its maximum value in the region near the plate and decreases properly on increasing boundary layer coordinate η to attain free-stream value. The thickness of the boundary layer decreases on increasing t_1 and M^2 whereas it increases on increasing m, G_r, N_r and t. It is worthy to note that, for ramped temperature plate, time t is always less or equal to than t_1 i.e. $t \leq t_1$. Due to this reason $t = 0.9$ is considered in Figs. 4 and 10 in place of $t = 1.4$ which is considered in other figures.

The numerical values of rate of heat transfer at plate i.e. $(\partial T/\partial\eta)_{\eta=0}$, computed from the analytical expression (4.1), are presented in tabular form in Tables 1–3 for various values of N_r, φ, t and t_1 taking $P_r = 0.71$. It is evident from Tables 1 and 2 that $(\partial T/\partial\eta)_{\eta=0}$ decreases on increasing N_r and t_1 whereas it increases on increasing φ. This implies that thermal radiation and critical time for rampedness tend to reduce rate of heat transfer at the plate whereas heat absorption has a reverse effect on it. It is noticed from Table 3 that $(\partial T/\partial\eta)_{\eta=0}$ increases on increasing t. This implies that rate of heat transfer at plate is getting enhanced with the progress of time. It is interesting to note form Table 3 that rate of heat transfer approaches steady state with the progress of time when $t \geq 3.2$ $(t > t_1)$.

The numerical values of primary shear stress τ_x and secondary shear stress τ_z at the plate, computed from the analytical expression (5.1), are displayed in tabular form in Tables 4–7 for various values of M^2, m, G_r, N_r, φ, t and t_1 taking $a = 1$ and $P_r = 0.71$. It is evident form Tables 4–7 that primary shear

Table 4 Shear stress at the plate when $G_r = 6$, $t_1 = 2$, $N_r = 2$, $\varphi = 3$ and $t = 1.4$.

	$M^2 \rightarrow$ $m \downarrow$	10	15	20
$-\tau_x$	0.5	3.2105	4.2404	5.0889
	1.0	2.5058	3.4027	4.1374
	1.5	1.8923	2.6804	3.3216
τ_z	0.5	1.0923	1.3030	1.4789
	1.0	1.6518	1.9665	2.2270
	1.5	1.8443	2.1940	2.4799

Table 5 Shear stress at the plate when $m = 0.5$, $M^2 = 10$, $t_1 = 2$, $N_r = 2$, and $\varphi = 3$.

	$t \rightarrow$ $G_r \downarrow$	1.0	1.4	1.8	3.0	3.2	3.4
$-\tau_x$	6	2.3555	3.2105	4.0655	7.3482	7.9302	8.5123
	8	2.1162	2.8681	3.6200	6.8326	7.4147	7.9968
	10	1.8769	2.5258	3.1745	6.3171	6.8991	7.4812
τ_z	6	0.7609	1.0923	1.4237	2.3060	2.4435	2.5809
	8	0.7983	1.1485	1.4988	2.4003	2.5378	2.6753
	10	0.8357	1.2047	1.5739	2.4946	2.6322	2.7697

Table 6 Shear stress at the plate when $m = 0.5$, $M^2 = 10$, $G_r = 6$, $t_1 = 2$, and $t = 1.4$.

	$\varphi \rightarrow$ $N_r \downarrow$	1	3	5
$-\tau_x$	2	3.1373	3.2105	3.2617
	4	3.0932	3.1554	3.1997
	6	3.0685	3.1237	3.1635
τ_z	2	1.1170	1.0923	1.0758
	4	1.1338	1.1116	1.0963
	6	1.1436	1.1232	1.1090

Table 7 Shear stress at the plate when $m = 0.5$, $M^2 = 10$, $G_r = 6$, $\varphi = 3$ and $t = 0.9$.

	$N_r \rightarrow$ $t_1 \downarrow$	2	4	6
$-\tau_x$	1.0	1.5010	1.4292	1.3878
	1.5	1.9281	1.8803	1.8526
	2.0	2.1417	2.1058	2.0851
τ_z	1.0	0.7762	0.7998	0.8142
	1.5	0.7108	0.7266	0.7361
	2.0	0.6781	0.6899	0.6971

stress τ_x increases on increasing M^2, φ, t and t_1 whereas it decreases on increasing m, G_r, and N_r. Secondary shear stress τ_z increases on increasing M^2, m, G_r, t and N_r whereas it decreases on increasing φ and t_1. This implies that magnetic field, heat absorption, time and critical time for rampedness tend to enhance primary shear stress at the plate whereas Hall current, thermal buoyancy force and thermal radiation have reverse effect on it. Magnetic field, Hall current, thermal buoyancy force and time tend to enhance secondary shear stress at the plate whereas heat absorption and critical time for rampedness have reverse effect on it.

7. Conclusions

An investigation of unsteady hydromagnetic free convection flow with Hall effects of a viscous, incompressible, electrically conducting, optically thick radiating and heat absorbing fluid past a uniformly accelerated moving vertical plate with variable ramped temperature is carried out. Significant findings of the problem are mentioned below:

- Fluid temperature is getting reduced on increasing critical time for rampedness whereas thermal radiation and time have reverse effect on it. Fluid temperature approaches steady state when $t \geq 3.2$ $(t > t_1)$.
- Magnetic field tends to decelerate fluid flow in both the primary and secondary flow directions whereas Hall current, thermal buoyancy force, thermal radiation and time have reverse effect on it. Fluid flow in both the primary and secondary flow directions is getting decelerated on increasing critical time for rampedness.
- Thermal radiation and critical time for rampedness tend to reduce rate of heat transfer at the plate whereas heat absorption has a reverse effect on it. Rate of heat transfer at the plate is getting enhanced with the progress of time and it approaches steady state when $t \geq 3.2$ $(t > t_1)$.
- Magnetic field, heat absorption, time and critical time for rampedness tend to enhance primary shear stress at the plate whereas Hall current, thermal buoyancy force and thermal radiation have reverse effect on it. Magnetic field, Hall current, thermal buoyancy force and time tend to enhance secondary shear stress at the plate whereas heat absorption and critical time for rampedness have reverse effect on it.

Acknowledgment

Authors are grateful to the reviewers for their valuable suggestions which helped us to improve the quality of this research paper. Authors are also thankful to Indian School of Mines, Dhanbad for providing financial support to carry out this research work.

References

[1] J.R. Howell, R. Siegel, M.P. Menguc, Thermal Radiation Heat Transfer, 5th ed., CRC Press, New York, 2010.
[2] A.J. Chamkha, Thermal radiation and buoyancy effects on hydromagnetic flow over an accelerating permeable surface with heat source or sink, Int. J. Eng. Sci. 38 (2000) 1699–1712.
[3] E.M.A. Elbashbeshy, T.G. Emam, Effects of thermal radiation and heat transfer over an unsteady stretching surface embedded in a porous medium in the presence of heat source or sink, Therm. Sci. 15 (2011) 477–485.
[4] D. Pal, Combined effects of non-uniform heat source/sink and thermal radiation on heat transfer over an unsteady stretching permeable surface, Commun. Nonlinear Sci. Numer. Simul. 16 (2011) 1890–1904.
[5] O.D. Makinde, Heat and mass transfer by MHD mixed convection stagnation point flow toward a vertical plate embedded in a highly porous medium with radiation and internal heat generation, Meccanica 47 (2012) 1173–1184.
[6] P. Chandran, N.C. Sacheti, A.K. Singh, Natural convection near a vertical plate with ramped wall temperature, Heat Mass Transf. 41 (2005) 459–464.
[7] V. Rajesh, Radiation effects on MHD free convection flow near a vertical plate with ramped wall temperature, Int. J. Appl. Math. Mech. 6 (2010) 60–77.
[8] Samiulhaq, I. Khan, F. Ali, S. Shafie, MHD free convection flow in a porous medium with thermal diffusion and ramped wall temperature, J. Phy. Soc. Jpn 81 (2012) 044401 http://dx.doi.org/10.1143/JPSJ.81.044401.
[9] K. Das, Magnetohydrodynamics free convection flow of a radiating and chemically reacting fluid past an impulsively moving plate with ramped wall temperature, J. Appl. Mech. 79 (2012) 061017, doi:10.1115/1.4006462.
[10] R. Nandkeolyar, M. Das, MHD free convective radiative flow past a flat plate with ramped temperature in the presence of an inclined magnetic field, Comp. Appl. Math. 34 (2015) 109–123, doi:10.1007/s40314-013-0107-6.
[11] R. Nandkeolyar, P. Sibanda, Md.S. Ansari, Unsteady hydromagnetic radiative flow of a dusty fluid past a porous plate with ramped wall temperature, Proceedings of the Annual ASME International Mechanical Engineering Congress and Exposition, 7A, 2013, doi:10.1115/IMECE2013-66699.
[12] P.K. Kundu, K. Das, N. Acharya, Flow features of a conducting fluid near an accelerated vertical plate in porous medium with ramped wall temperature, J. Mech. 30 (2014) 277–288.
[13] G.S. Seth, S.M. Hussain, S. Sarkar, Hydromagnetic natural convection flow with heat and mass transfer of a chemically reacting and heat absorbing fluid past an accelerated moving vertical plate with ramped temperature and ramped surface concentration through a porous medium, J. Egypt. Math. Soc. 23 (2015) 197–207.
[14] I. Pop, T. Watanabe, Hall effects on magnetohydrodynamic free convection about a semi-infinite vertical flat plate, Int. J. Eng. Sci. 32 (1994) 1903–1911.
[15] E.M. Aboeldahab, E.M.E. Elbarbary, Hall current effect on magnetohydrodynamic free convection flow past a semi-infinite vertical plate with mass transfer, Int. J. Eng. Sci. 39 (2001) 1641–1652.
[16] G.S. Seth, S. Sarkar, G.K. Mahato, Effects of Hall current on hydromagnetic free convection flow with heat and mass transfer of a heat absorbing fluid past an impulsively moving vertical plate with ramped temperature, Int. J. Heat Tech. 31 (2013) 85–96.
[17] S. Das, B.C. Sarkar, R.N. Jana, Hall effect on MHD free convection boundary layer flow past a vertical flat plate, Meccanica 48 (2013) 1387–1398.
[18] K.R. Cramer, S.I. Pai, Magnetofluid Dynamics for Engineers and Applied Physicists, McGraw Hill Book Company, New York, USA, 1973.